Control of Molecular orientation and alignement by monotonic schemes

Julien Salomon, Gabriel Turinici

CONTROL OF MOLECULAR ORIENTATION AND ALIGNMENT BY MONOTONIC SCHEMES

Salomon Julien
Laboratoire Jacques-Louis Lions
Universit Pierre & Marie Curie
Boite courrier 187, 75252 Paris Cedex 05
France
email: Salomon@ann.jussieu.fr

Gabriel Turinici
INRIA Rocquencourt, B.P. 105, 78153 Le Chesnay Cedex
and
CERMICS-ENPC, Champs sur Marne, 77455 Marne la valle Cedex
France
email: Gabriel.Turinici@inria.fr

ABSTRACT
Many numerical simulations in quantum (bilinear) control use monotonically convergent algorithms. A relevant time discretization has already been proposed for these algorithms. We present here a way to apply these algorithms to the control of molecular orientation and alignment. Numerical results that illustrate some of the properties of these algorithms are given.

KEY WORDS
Quantum control, monotonically convergent schemes, molecular orientation and alignment, bilinear control, laser pulse shape designing.

1 Introduction

Laser control of complex molecular systems is becoming feasible, especially since the introduction [1] [2] of closed loop laboratory learning techniques and their successful implementation [3, 4, 5, 6, 7, 8]. Among all possibilities provided by this technique, control of molecular alignment and orientation is not only a major concern in chemical reaction dynamics as an efficient cross-section enhancement device [9, 10, 11, 12] but may also become a determinant technique in controlling surface processing [13], catalysis [14] and for nanoscale design by laser focusing of molecular beams [13, 15].
At the level of the numerical simulations, the introduction of the monotonically convergent algorithms the Zhu & Rabitz [16] that extends an algorithm due to Krotov [17] has allowed a considerable progress and made possible further investigations in this area. Recently, a general class of monotonically convergent algorithms has been proposed [18] and relevant time discretization has been developed [19].
Although numerical simulation of the rotation control have already been demonstrated [20, 21] the use of monotonic schemes has not been tested so far. In this paper we propose and test on an example monotonic schemes to design laser pulses to control alignement or orientation of molecules. The contents of the paper is as follows : the physical model is described in Section 2 ; the necessary background and definitions of the quantum control settings are given in the Section 3 ; the monotonic scheme adpated to the orientation control is presented in Section 4 followed by some numerical results in Section 5.

2 Model

Let us consider the HCN molecule in its ground electronic state as a rigid rotor interacting with an electric field ε. This system can be described as a permanent dipole μ_0 with polarizability components $\alpha_{\|}$, $\alpha_{\perp}$.
The Hamiltonian of this system is

$$\begin{aligned} H &= B\mathcal{J} - \mu_0\varepsilon(t)\cos\theta \\ &\qquad -\tfrac{\varepsilon^2(t)}{2}(\alpha_{\|}\cos^2\theta + \alpha_{\perp}\sin^2\theta) \\ &= B\mathcal{J} - \mu_0\varepsilon(t)\cos\theta - \tfrac{\varepsilon^2(t)}{2}(\Delta\alpha\cos^2\theta + \alpha_{\perp}), \end{aligned}$$

where $\mathcal{J}$ is the angular-momentum operator defined by :

$$\mathcal{J} = \frac{-\hbar^2}{\sin\theta}\frac{\partial}{\partial\theta}\Big(\sin\theta\frac{\partial}{\partial\theta}\Big),$$

B the rotational constant, θ the polar angle that defines orientation of the molecule with respect to the linearly polarized electric-field vector $\vec{\varepsilon}$ at the time t and where $\Delta\alpha = \alpha_{\|} - \alpha_{\perp}$. The time evolution of an initial distribution $\psi(\theta, \phi; t = 0)$ is governed by the time-dependent Schrödinger equation :

$$i\hbar\partial_t\psi(\theta,\phi;t) = H\psi(\theta,\phi;t),$$

with the azimuthal angle. In what follows this angle will be taken as 0 because of the conservation of the laboratory axis symmetry.
Numerical computations will be done in the basis of the eigen vectors of $\hat{J}$ that are the spherical harmonics :

$$Y_J(\theta) = \sqrt{\frac{2J+1}{4\pi}}P_J(\cos\theta),$$

where P_J stands for the J-th Legendre-polynomial.

3 Quantum control setting

3.1 Cost functional

The optimal control framework is then introduced to find a suitable evolution of $\varepsilon(t)$ over the control time interval $[0, T]$. The goal that the final state $\psi(T)$ has prescribed properties is expressed by the introduction of a cost functional J to be maximized. This cost functional also includes a contribution that penalizes undesirable effects. Let us consider thus the following functional :

$$J(\varepsilon) =< \psi(T)|O|\psi(T) > - \int_0^T \lambda(t)\varepsilon^2(t)dt,$$

where O is an observable operator that encodes the goal, i.e. $\cos\theta$ for the control of orientation case or $\cos^2\theta$ for the control of alignment case and $\lambda(t)$ the penalization parameter of the electric field. For reasons that will appear later, we will work with $\cos\theta + Id$ and $\cos^2\theta + Id$ which makes the operator O positive and does not modify extrema of J.

3.2 Euler equations and adjoint state

At the maximum of the cost functional $J(\varepsilon)$, the Euler-Lagrange critical point equations are satisfied ; a standard way to write these equations is to use a Lagrange multiplier $\chi(\theta, t)$ called *adjoint state*. The following critical point equation are thus obtained :

$$\begin{aligned} i\partial_t\psi &= H\psi, \quad \psi(0) = \psi_0 \\ i\partial_t\chi &= H\chi, \quad \chi(T) = O(\psi(T)) \\ \lambda(t)\varepsilon(t) &= -\Im < \chi|\mu_0.\cos\theta \\ &\quad +2\varepsilon(t).(\Delta\alpha\cos^2\theta + \alpha_\perp)|\psi >, \end{aligned} \tag{1}$$

where $\Im$ is the imaginary part of a complex number.

4 Monotonic scheme

4.1 Principle of the scheme

Let us consider two electric fields $\varepsilon_1(t)$ and $\varepsilon_2(t)$, the corresponding states ψ_1, ψ_2 and adjoint states χ_1, χ_2 computed by (1). The following computation allows us to elaborate monotonic schemes [16, 18]. Let us evaluate difference between $J(\varepsilon_1(t))$ and $J(\varepsilon_2(t))$:

$$\begin{aligned} \Delta J &= J(\varepsilon_2) - J(\varepsilon_1) \\ &= < \psi_2(T) - \psi_1(T)|O|\psi_2(T) - \psi_1(T) > \\ &\quad +2\Re < \psi_2(T) - \psi_1(T)|O|\psi_1(T) > \\ &\quad - \int_0^T \lambda(t)(\varepsilon_2^2(t) - \varepsilon_1^2(t))dt. \end{aligned}$$

Here $\Re$ is the real part of a complex number. Focusing on the term $< \psi_2(T) - \psi_1(T)|O|\psi_1(T) >$, we find :

$$\begin{aligned} &< \psi_2(T) - \psi_1(T)|O|\psi_1(T) >= \\ &\qquad < \psi_2(T) - \psi_1(T)|\chi_1(T) > \\ &= \int_0^T \big(< \partial_t(\psi_2(t) - \psi_1(t))|\chi_1(t) > \\ &\qquad + < \psi_2(t) - \psi_1(t)|\partial_t\chi_1(t) > \big)dt \\ &= i\int_0^T \big((\varepsilon_1(t) - \varepsilon_2(t)) < \psi_2(t)|\mu_0\cos\theta|\chi_1(t) > \\ &+(\varepsilon_1^2(t) - \varepsilon_2^2(t)) < \psi_2(t)|\tfrac{\Delta\alpha\cos^2\theta+\alpha_\perp}{2}|\chi_1(t) > \big)dt. \end{aligned}$$

Finally ΔJ can be evaluated by the formulae :

$$\begin{aligned} \Delta J =& < \psi_2(T) - \psi_1(T)|O|\psi_2(T) - \psi_1(T) > \\ &+\int_0^T (\varepsilon_2(t) - \varepsilon_1(t))\Big(\Im < \psi_2(t)|\mu_0\cos\theta|\chi_1(t) > \\ &\qquad +(\varepsilon_2(t) + \varepsilon_1(t)) \\ &\qquad .\big(\Im < \psi_2(t)|\tfrac{\Delta\alpha\cos^2\theta+\alpha_\perp}{2}|\chi_1(t) > -\lambda(t)\big)\Big)dt \end{aligned}$$

The first term of this sum is positive since $O = \cos + Id$ or $O = \cos^2 + Id$. Given ε_1, the integrant provides thus an implicit criterium in terms of ε_2, the satisfaction of which guaranties the positivity of ΔJ. Let us make explicit the choice of ε_2 : the integrant is second order polynomial with respect to ε_2 and for a large enough value of $\lambda(t)$ the coefficient $\Im < \psi_2(t)|\frac{\Delta\alpha\cos^2\theta+\alpha_\perp}{2}|\chi_1(t) > -\lambda(t)$ of $\varepsilon_2^2(t)$ is negative. It has thus a unique maximum, given by the cancellation of the derivative. The value obtained by this method is :

$$\varepsilon_2(t) = -\frac{\Im < \psi_2(t)|\mu_0\cos\theta|\chi_1(t) >}{2\Im < \psi_2(t)|\frac{\Delta\alpha\cos^2\theta+\alpha_\perp}{2}|\chi_1(t) > -\lambda(t)}.$$

4.2 Algorithm

The algorithm derived from the previous computations is then given by the following statements : given at step k a field ε^k and its associated state ψ^k and adjoint state χ^k, compute simultaneously $\varepsilon^{k+1}, \psi^{k+1}$ by

$$\begin{cases} \varepsilon^{k+1} = -\frac{\Im<\psi_{k+1}(t)|\mu_0\cos\theta|\chi_k(t)>}{2\Im<\psi_{k+1}(t)|\frac{\Delta\alpha\cos^2\theta+\alpha_\perp}{2}|\chi_k(t)>-\lambda(t)} \\ i\partial_t\psi^{k+1} = (B - \mu_0\varepsilon^{k+1}(t)\cos\theta \\ \qquad -\frac{(\varepsilon^{k+1})^2(t)}{2}(\Delta\alpha\cos^2\theta + \alpha_\perp)\psi^{k+1} \\ \psi^{k+1}(0,\theta) = \psi_0(\theta). \end{cases}$$

Then compute backward evolution of χ^{k+1} by :

$$\begin{cases} i\partial_t \chi^{k+1} &= (B - \mu_0 \varepsilon^{k+1}(t)\cos\theta \\ & \quad - \frac{(\varepsilon^{k+1})^2(t)}{2}(\Delta\alpha \cos^2\theta + \alpha_\perp)\chi^{k+1} \\ \chi^{k+1}(T,\theta) &= O(\psi^{k+1}(T,\theta)). \end{cases}$$

The arguments above show that :

$$J(\varepsilon^{k+1}) \geq J(\varepsilon^k).$$

4.3 Remark on time discretization

The proposed algorithm contains implicit computations. Indeed the value of $\varepsilon^{k+1}(t)$ has to be known to compute $\psi^{k+1}(t)$. We have presented in [19] time discretizations of this scheme that cancels out the implicit steps and maintains the monotonicity with respect to the time discretized cost functionnal $J_{\Delta T} =< \psi_N|O|\psi_N > -\Delta T \sum_0^N \lambda_j \varepsilon_j^2$, where the sequences (ψ_j) and (ε_j) stand for discrete representations of $\psi(t)$ and $\varepsilon(t)$.

5 Numerical results

The values of the parameters we have used to test the algorithm are the one of [20] which describe the HCN molecule.

B	μ	$\alpha_\parallel$	$\alpha_\perp$
6.6376×10^{-6}	1.1413	20.055	8.638

Time control has been chosen with respect to the value of the first transition of the system without laser excitation, i.e. $T_0 = \frac{2\pi}{B} = 9.4660 \times 10^5$.
The software Octave has been used to perform numerical computations. Two cases have then been tested : control on $[0, T_0]$ and on $[0, 10T_0]$ for both observables $O = \cos\theta + Id$ and $O = \cos^2\theta + Id$. Numerical simulations have been performed in the basis of the first ten eigen vectors of the internal Hamiltonian and the first of them has been taken as initial value ψ_0. Even though the scheme is explicit, a good time stability has been observed since tests with $dT = 10^4$ have provided fields looking like the ones obtained with $dT = 10^2$. It has been decided to strongly penalize the electric field at the beginning of the control interval to satisfy physical restrictions.

5.1 Control on $[0, T_0]$

Figures below represent the values of the state $\psi(\theta, T_0)$ with respect to θ and of the corresponding electrical field of control $\varepsilon(t)$. These fields, corresponding to $O = \cos\theta + Id$ and $O = \cos^2\theta + Id$ have been obtained after 500 iterations of the monotonic scheme, but, dependant on the quality requested, fewer number of iteration can be used.

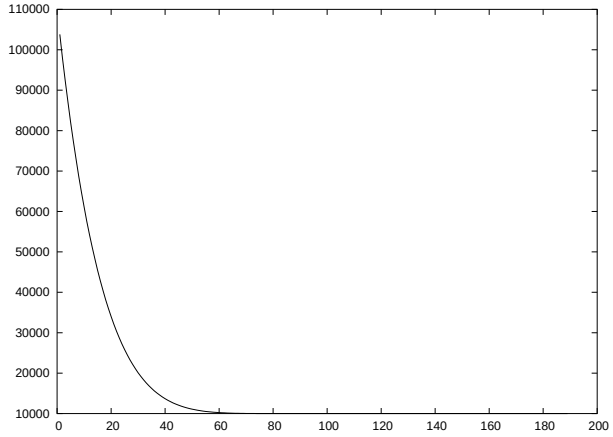

Figure 1. Value of λ with respect to the number of time step. This coeffi cient of penalization is defi ned as $\lambda(t) = 10^5(\frac{t-T/2}{T/2})^6 + 10^4$ if $t < T/2$ and $\lambda(t) = 10^4$ in the other case.

5.1.1 Control of orientation

The control obtained enables us to localize of the state around the angular values 0 and 2π. The evolution of the cost functional and of the observable $< \psi(\theta, T_0)|\cos\theta|\psi(\theta, T_0 >$ have also been represented.

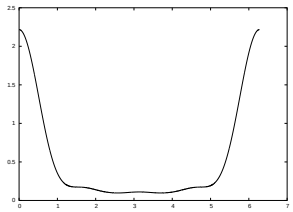

Figure 2. State $|\psi(\theta, T_0)|$ with respect to the number of time step.

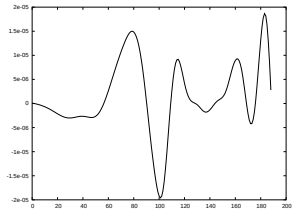

Figure 3. Electric fi eld $\varepsilon(t)$ with respect to the number of time step.

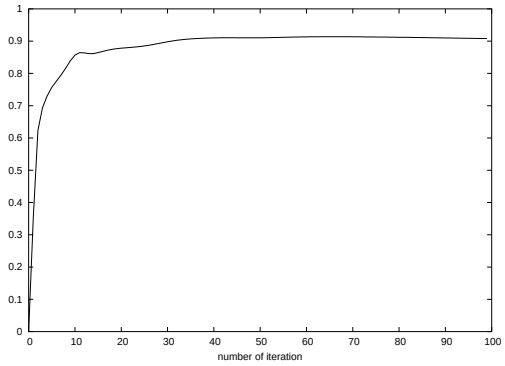

Figure 4. Value of the observable $< \psi(T_0)|\cos\theta|\psi(\theta, T_0) >$ over 100 fi rst iterations.

The value of $< \psi(\theta, T_0)|\cos\theta|\psi(\theta, T_0) >$ is equal to 1.91 after 100 iterations.

5.1.2 Control of alignment

The control obtained enable the localization of the state around the angular values 0, π and 2π.

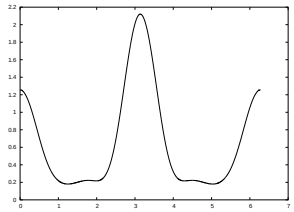

Figure 5. $|\psi(\theta, T_0)|$. Here $< \psi(\theta, T_0)|\cos^2\theta|\psi(\theta, T_0) >$ is near 0.88 after about 200 iterations.

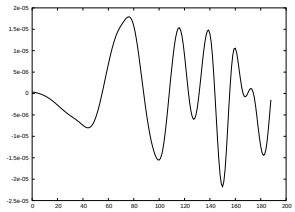

Figure 6. Electric field $\varepsilon(t)$ with respect to the number of time step.

5.2 Control on $[0, 10T_0]$

5.2.1 Control of orientation

Figures below represent the values of the state $\psi(\theta, 10T_0)$ with respect to θ and of the corresponding electrical field of control $\varepsilon(t)$. In this case only 30 iterations of the monotonic scheme were necessary.

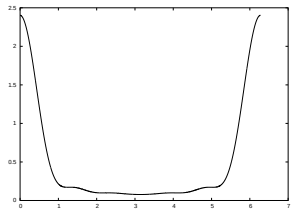

Figure 7. $|\psi(\theta, 10T_0)|$. Here $<\psi(\theta, 10T_0)|\cos\theta|\psi(\theta, 10T_0)>$ is near 0.94.

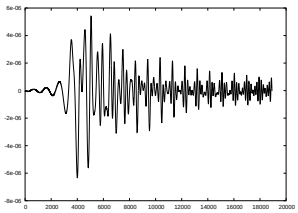

Figure 8. Electric field $\varepsilon(t)$ with respect to the number of time step.

5.2.2 Control of alignement

Figures below represent the values of the state $\psi(\theta, 10T_0)$ with respect to θ and of the corresponding electrical field of control $\varepsilon(t)$. About 100 iterations were performed.

5.3 Kicks

For certain choices of $\lambda(t)$, computations leads to kick-like fields, which have physical interest because of their simplicity [20]. Some examples of such fields have been represented above for a control on $[0, T_0]$: The value of 0.97 is reached by the observable $< \psi(\theta, 10T_0)|\cos^2\theta|\psi(\theta, 10T_0) >$ in these cases. This result is better than the one obtained with the penalization of Fig.1. This fact can be explained by the lower values of $\lambda(t)$ we have used here.

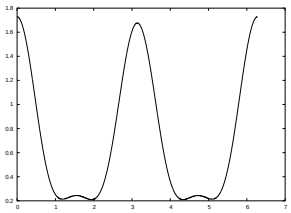

Figure 9. $|\psi(\theta, 10T_0)|$. Here $<\psi(\theta, 10T_0)|\cos^2\theta|\psi(\theta, 10T_0)>$ is near 0.87.

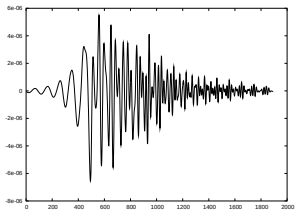

Figure 10. Electric field $\varepsilon(t)$ with respect to the number of time step.

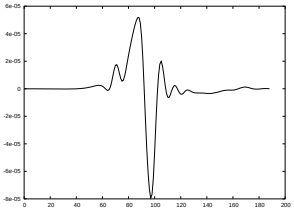

Figure 11. Electric field $\varepsilon(t)$ with respect to the number of time step.

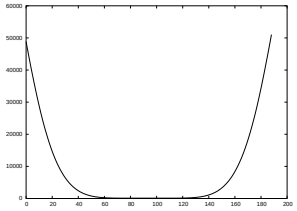

Figure 12. Value of $\lambda(t)$ with respect to the number of time step.

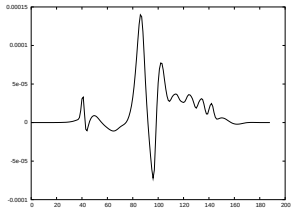

Figure 13. Electric field $\varepsilon(t)$ with respect to the number of time step.

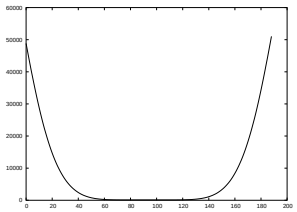

Figure 14. Value of $\lambda(t)$ with respect to the number of time step.

References

[1] R. S. Judson and H. Rabitz, Teaching lasers to control molecules, *Phys. Rev. Lett.*, 68, 1992, 1500-1503.

[2] S. Shi, A. Woody, and H. Rabitz, Optimal control of selective vibrationnal excitation in harmonic linear chain molecules, *J. Chem. Phys.*, 88, 1988, 6870-6883.

[3] R. J. Levis, G. Menkir and H. Rabitz, Selective bond dissociation and rearrangement with optimal tailored, *Science*, 292, 2001, 709-713.

[4] A. Assion, T. Baumert, M. Bergt, T. Brixner, B. Kiefer, V. Seyfried, M. Strehle and G. Gerber, Control of chemical reactions by feedback-optimized phase-shaped femtosecond laser pulses, *Science*, 282, 1998, 919-922.

[5] M. Bergt, T. Brixner, B. Kiefer, M. Strehle and G. Gerber, Controlling the femto-chemistry of $Fe(CO)_5$, *J. Phys. Chem. A.*, 103, 1999, 10381-10387.

[6] T. Weinacht, J. Ahn and P. Bucksbaum, Controlling the shape of a quantum wavefunction, *Nature*, 397, 1999, 233-235.

[7] C. Bardeen, V. V. Yakovlev, K. R. Wilson, S. D. Carpenter, P. M. Weber and W. S. Warren, Feedback quantum control of molecular electronic population transfert, *Chem. Phys. Lett.*, 280, 1997, 151-158.

[8] C. J. Bardeen, V. V. Yakovlev, J. A. Squier and K. R. Wilson, Quantum control of population transfer in green flourescent protein by using chirped femtosecond pulses. *J. Am. Chem. Soc.*, 120, 1998, 13023-13027.

[9] P. R. Brooks, Reactions of oriented molecules, *Science*, 193, 1976.

[10] A. H. Zewail, Femtochemistry : the role of alignment and orientation, *J. Chem. Soc., Faraday Trans. 2*, 85, 1989, 1221.

[11] H. J. Loesch and A. Remscheid, Brute force in molecular reaction dynamics: A novel technique for measuring steric effects, *J. Chem. Phys.*, 93, 1990, 4779-4790.

[12] F. J. Aoiz, B. Friedrich, V. J. Herrero, V. S. Rábanos and J. E. Verdasco, Effect of pendular orientation on the reactivity of H + DCl: a quasiclassical trajectory study, *Chem. Phys. Lett.*, 289, 1998, 132-140.

[13] T. Seidman, Molecular optics in an intense laser field: A route to nanoscale material design, *Phys. Rev. A*, 56, 1997, R17-R20.

[14] J. Bulthuis, J. B. Milan, M. H. M. Janssen, and S. Stolte, Electric field dependence of reactivity of state-selected and oriented methylhalides *J. Chem. Phys.*, 94(11), 1991, 7181-7192.

[15] H. Stapelfeldt, H. Sakai, E. Constant and P. B. Corkum, Deflection of Neutral Molecules using the Nonresonant Dipole Force, *Phys. Rev. Lett.*, 79, 1997, 2787-2790.

[16] W. Zhu and H. Rabitz, A rapid monotonically convergent iteration algorithm for quantum optimal control over the expectation value of a positive definite operator, *J. Chem. Phys.*, 109, 1998, 385-391.

[17] D. Tannor, V. Kazakov and V. Orlov, Control of photochemical branching : Novel procedures for finding optimal pulses and global upper bounds, in J. Broeckhove and L. Lathouwers (Ed.) *Time Dependent Quantum Molecular Dynamics*, (Plenum, 1992) 347-360.

[18] Y. Maday and G. Turinici, New formulations of monotonically convergent quantum control algorithms, *J. Chem. Phys.*, 118, 2003, 8191-8196.

[19] Yvon Maday, Julien Salomon, and Gabriel Turinici, Discretely monotonically convergent algorithms in quantum control, *Prooceedings of the LHMNLC03 IFAC conference*, Sevilla, Spain, 3-5 April 2003, 321-324.

[20] C. Dion, A. Ben Haj-Yedder, E. Cancs, C. Le Bris, A. Keller, O. Atabek, Optimal laser control of orientation : The Kicked molecule, *Phys. Rev. A*, 65, 2002, 063408-1 063408-7.

[21] C. Dion, A. Ben Haj-Yedder, E. Cancs, C. Le Bris, A. Keller, O. Atabek, Numerical optimization of laser fields to control molecular orientation, *Phys. Rev. A*, 66, 2002, 063401-1 063401-9.